Edge-Assisted Sensor Control in Healthcare IoT

Delaram Amiri[1], Arman Anzanpour[2], Iman Azimi[2], Marco Levorato [1], Amir M. Rahmani[1,3], Pasi Liljeberg[2], and Nikil Dutt[1]
[1]Department of Electrical Engineering and Computer Science, University of California Irvine, USA
[2]Department of Future Technologies, University of Turku, Finland
[3]Institute for Computer Technology, TU Wien, Vienna, Austria
{damiri, levorato, amirr1, dutt}@uci.edu, {armanz, imaazi, pakrli}@utu.fi

***Abstract*—The Internet of Things is a key enabler of mobile health-care applications. However, the inherent constraints of mobile devices, such as limited availability of energy, can impair their ability to produce accurate data and, in turn, degrade the output of algorithms processing them in real-time to evaluate the patient's state. This paper presents an edge-assisted framework, where models and control generated by an edge server inform the sensing parameters of mobile sensors. The objective is to maximize the probability that anomalies in the collected signals are detected over extensive periods of time under battery-imposed constraints. Although the proposed concept is general, the control framework is made specific to a use-case where vital signs – heart rate, respiration rate and oxygen saturation – are extracted from a Photoplethysmogram (PPG) signal to detect anomalies in real-time. Experimental results show a 16.9% reduction in sensing energy consumption in comparison to a constant energy consumption with the maximum misdetection probability of 0.17 in a 24-hour health monitoring system.**

***Index Terms*—Wearable Electronics, Internet of Things, Edge-Assisted Control, Energy Efficiency, Abnormality Detection**

I. Introduction

Recent advances in low-cost wearable sensing devices open new avenues to build innovative platforms for healthcare applications [1]. However, continuously collecting and processing physiological signals imposes a severe burden to inherently resource-constrained sensor nodes in terms of storage, computation load, and energy consumption. The 3-tier sensor-edge-cloud Internet of Things (IoT) architecture [2] can mitigate this issue by integrating the sensors within a larger – more capable – communication and processing infrastructure, where interconnected sensors can delegate some functionalities to edge or cloud devices [3]. However, healthcare applications that require high quality signals and high precision representations may still impose a considerable energy consumption to battery-powered sensors due to the need for continuous signal acquisition and data transmission.

Various approaches to reduce the energy consumption of sensors have been proposed in prior literature, including sensor sleep scheduling [4], [5], [6] and power aware cognitive communication protocols [7]. [8], [9] mainly focus on the optimization of the energy used by the sensor node to transmit the collected signal. One of the key contributions of our work is the development of an edge-assisted framework for the dynamic control of *sensing energy*, and thus accuracy, as a function of the current "context", here defined as the activity of the monitored person. Related to the present work, activity-based optimization frameworks was proposed in [10], [11], [12]. However, the objective of these frameworks, based on Markov Decision Process theory, is that of detecting the activity itself. Furthermore, their main assumption is that the gateway – a smartphone in their scenario – is the energy bottleneck of the system. In contrast, our approach uses the estimated activity to control sensing accuracy in an edge-based architecture to maximize the lifetime of the sensor.

Our overall objective is to dynamically adapt sensing accuracy, and thus the energy consumption, to maximize the sensor's lifetime. The key idea behind our approach is that different "contexts" in which the signal is captured, require different energy levels to achieve a certain accuracy of estimation and/or detection. Thus, a context-aware adaptation at run-time can possibly reduce energy expense while meeting a predefined performance of signal analysis. A critical challenge, then, is to build an effective analysis loop which enables such adaptation. Due to limited processing capabilities and partial view of the system, sensors are not typically suitable devices to extract context and perform optimization. At the other end of the infrastructure, cloud servers have sufficient computation power and a global view, but typically incurs a large, and unpredictable, delay due to multi-hop data propagation through the Internet. Topological as well as geographic proximity of sensors and edge servers grants a fast response time of the system [13], making edge servers a perfect location to host multi-sensor analysis and optimization algorithms.

We apply our approach to a use-case focused on the detection of abnormalities in the vital signs extracted from Photoplethysmogram (PPG) signals. PPG is an optical signal presenting blood volume variations at the microvascular level [14] which allows the estimation of vital signs such as heart rate, heart rate variability, respiration rate and blood oxygen saturation (SpO_2). PPG measurements are obtained using a non-invasive and low-cost miniaturized sensor which can be integrated in wearable sensors (e.g., fitness trackers, smart watches) to continuously capture vital signs.

Importantly, the noise level of the captured signal is sensitive to the monitored subject's activity (e.g., "Sleeping" or "Running"). For instance, noise during "Sleeping" state is significantly smaller to that during "Running". Thus, a considerably smaller energy budget can be used to achieve the same estimation accuracy when acquiring the signal in the former case compared to the latter. Additionally, the monitored

978-1-5386-4727-1/18/$31.00 ©2018 IEEE

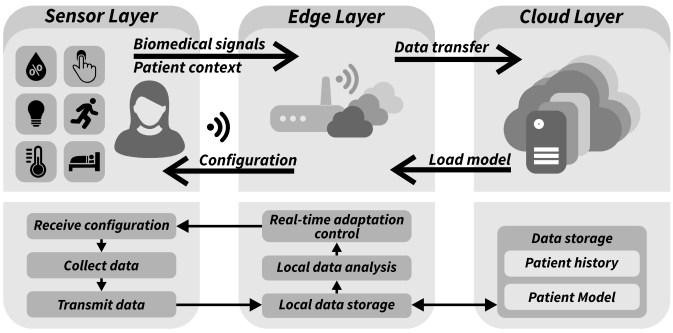

Fig. 1: The upper part of the figure shows the system architecture while the lower part shows the closed loop of interactions between the sensor, edge, and cloud layers.

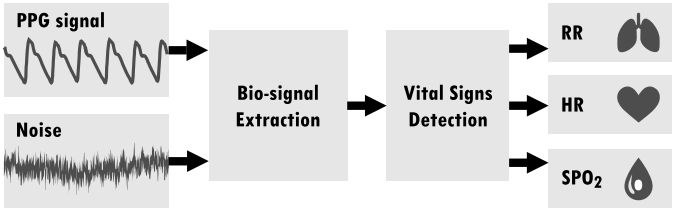

Fig. 2: Local data analysis to extract vital signs from raw PPG signals.

subject's activity can influence the "abnormal" region of vital parameters: a person "Sitting" has a smaller baseline heart rate compared to the same person "Running". Using real-world data collected using a PPG-based sensor node, we show that our framework, by adapting the sensing parameters based on the activity, can reduce sensing energy consumption by 16.9% over a daily cycle compared to the non-adaptive case meeting a predefined threshold of maximum detection error.

The rest of the this paper is organized as follows. Section II describes the layered architecture of the system. The monitoring and detection frameworks are presented in Section III. Section IV presents and discusses numerical results, and Section V concludes the paper.

II. System Architecture

Herein, we present the 3-layer (sensor-edge-cloud) structure of the proposed , with the edge layer enabling system adaptivity in real-time, illustrated in Figure 1.

The edge layer controls the configuration used by the sensor to acquire the signal, which is transmitted to the edge processor. The gateway device in the edge layer stores collected data temporarily and performs a local analysis to extract the context, which is then used to determine a new configuration. This procedure realizes a closed-loop control which dynamically adapts the sensing parameters to the context. The cloud server receives the data and builds and maintains a signal model used to optimize the configuration at the edge layer.

Case Study: PPG Sensor-based IoT system

We now present a case study of the deployed PPG sensor-based IoT system, and begin by defining different layers of the 3-layer architecture.

Sensor layer: The sensor node is a wireless device which includes a PPG sensor, a wireless transmitter and a Micro-Controller Unit (MCU): i) The PPG sensor measures the reflection amplitude of infrared (IR) and red lights from the microvascular bed of tissues via two light emitter diodes (LEDs) and two light sensors, providing a 50 Hz-digitized signal through I_2C communication bus. ii) The wireless transmitter is a Wi-Fi module which enables communication to the edge layer to deliver the raw signals and receive configuration settings. iii) The MCU is an 80MHz 32-Bits RISC microprocessor with 96KB RAM. The microprocessor manages data collection, data writing on a 4MB QSPI flash memory and data transmission to the edge. The MCU is programmed to dynamically tune the current level of PPG sensor's LEDs (i.e., sensing setups) according to the configuration received from the edge processor upon request. In the recording mode, the PPG sensor uses five different current levels for driving the LEDs: 0.8mA, 3.5mA, 6.2mA, 9.3mA, and 12mA. Table I shows these current levels with their corresponding recording sensing power levels.

Edge layer: The gateway is a Linux-based device, providing three functionalities through an Apache web server.
1) Real-time adaptation control: this functionality aims at minimizing sensing power consumption while satisfying a predefined level of accuracy. The edge server receives context data and vital signs (e.g., heart rate, respiration rate and SpO_2) to generate configuration settings for the sensor layer.
2) Local data storage: the edge server receives data from the sensor layer, stores them in a MySQL database and periodically synchronizes with the cloud layer.
3) Local data analysis: the stored data are analyzed to extract heart rate, respiration rate and SpO_2 from the raw PPG signal, as well as the contextual information.

Local data analysis to extract vital signs can be partitioned into two main modules: *i) bio-signal extraction* and *ii) vital signs detection* [15] (see Figure 2):
i) Bio-signal extraction: Various techniques have been proposed to extract these bio-signals [15]. However, some of the existing techniques are not suitable to the considered application due to the presence of noise in the signal induced by some activities.

The respiratory signal can be obtained leveraging two main techniques, known as feature-based [16] and filter-based [17] extraction. Feature-based techniques derive certain features

TABLE I: System states with sensing power consumption

State	Power consumption
Recording mode: LEDs setting: 0.8mA	69.30mW
Recording mode: LEDs setting: 3.5mA	73.26mW
Recording mode: LEDs setting: 6.2mA	79.86mW
Recording mode: LEDs setting: 9.3mA	84.15mW
Recording mode: LEDs setting: 12mA	89.43mW

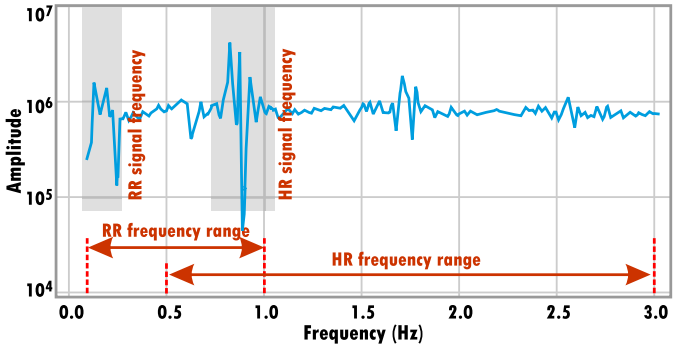

Fig. 3: Power Spectral Density (PSD) of one-minute PPG signal while the user is sleeping

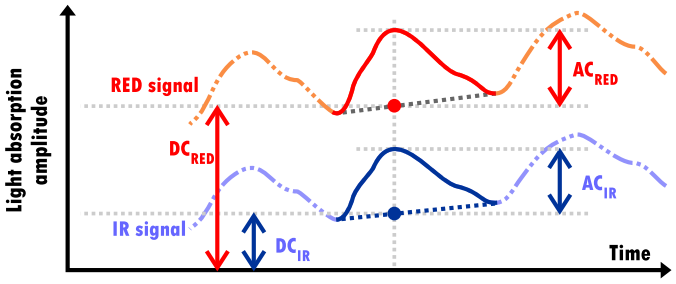

Fig. 4: Features in PPG signals for SpO_2 Calculation

such as pulse strength variations and baseline variations to derive the respiratory signal [16]. In contrast, filter-based techniques filter the raw signal to eliminate frequency components irrelevant to the respiratory signal [17]. Note that filter-based techniques can also be used to extract heartbeat signals.

In our system, we designed two band-pass filters (i.e., filter based techniques) to automatically extract respiratory and heartbeat signals during the monitoring period. We select the cutoff frequencies based on peak values in the power spectral density (PSD) of the PPG signal [18]. Figure 3 shows the PSD of a one-minute PPG signal while the user is sleeping. The peak in the heart rate frequency range (i.e., 0.5- 3.0 Hz) corresponds to heartbeat frequency, and the peak in respiration rate frequency range (i.e., 0.1-1 Hz) indicates respiratory frequency. Note that the respiration rate frequency range might contain the heart rate frequency peak (see Figure 3). Therefore, to extract the respiratory signal, first the heart rate frequency peak should be removed.

ii) Vital signs detection: A peak detection algorithm is applied to the filtered bio signals. The distance between two consecutive peaks corresponds to the respiration and heartbeat cycles. To estimate oxygen saturation (SpO_2), we extract 4 features from the IR and red signals (Figure 4). Then, SpO_2 is calculated as:

$$SpO_2 = AR^2 + BR + \Gamma, \quad R = \frac{AC_{RED}.DC_{IR}}{AC_{IR}.DC_{RED}}, \qquad (1)$$

where A, B and Γ are constants determined by the sensor's specification [19].

Cloud layer: The cloud layer is deployed on a Virtual Private Server (VPS) running an Apache web server on Ubuntu Linux operating system. The web server receives data from the edge layer, the OS file system stores collected data, and a MySQL database stores patient information and file indexes related to each patient, eventually creating a medical history of the patient and a model for her/his daily activities to be used in the edge layer for better state detection.

III. Real-Time Adaptation Framework

Our two-fold goal is to *minimize energy expense of the sensor node while satisfying the requirement in terms of abnormality detection*. Both the signal and the probability of an abnormal signal are function of the context, here defined as the following activities: "Sleeping", "Sitting", "Walking", "Jogging" and "Running". As the first step to formulate the optimization problem, we model the fidelity of sensor output as a function of the different activities and energy levels. In Section III-B, a Gaussian model for calculating error from vital signs is proposed. Section III-A discusses the method to solve the proposed optimization problem.

The first step is to evaluate the accuracy of the sensor compared to a ground truth signal in different operating conditions to build a model, which will be used to optimize the sensing energy. To this aim, the PPG signal from the sensor is preprocessed and the features oxygen saturation (SpO_2), heart rate, and respiration rate are evaluated for each combination of current level U and activity X. We use an ECG sensor as a reference for heart rate, an airflow sensor for respiration reference, and another PPG sensor with higher signal quality as a reference for SpO_2.

Based on this reference, we compute the error vectors of the three features: heart rate error $e_1(U,X)$, respiration rate error $e_2(U,X)$ and oxygen saturation error $e_3(U,X)$. We calculate the weighted total error vector $e(X,U) = \{\gamma_1 e_1(U,X) + \gamma_2 e_2(U,X) + \gamma_3 e_3(U,X)\}$. The variables $\gamma_1, \gamma_2, \gamma_3$ are positive weights such that $\gamma_1+\gamma_2+\gamma_3=1$. The control parameter U specifies the PPG sensor current. Note that the joint probability density function of error of extracted features as a result of activity state $X \in$ {Sleeping, Sitting, Walking, Jogging, Running} and current level $U \in \{U_1, U_2, ..., U_5\}$ follows $\rho(e(U,X) \mid U = u, X = x) \sim \mathcal{N}(0, \sigma(U,X))$. In this formulation, $\sigma(U,X)$ is the variance of error in the vector e given current level U and activity state X. In this case, the error probability can be calculated as the tail probability of the standard normal distribution as a function of the threshold T corresponding to the maximum total $RMSE$ in the estimated vital signs.

$$\mathcal{P}_{\text{error}}(T) = \int_{-\infty}^{T} \rho_E(e(U,X) \mid U = u, X = x)de \qquad (2)$$

A. Optimization

The model derived in the previous section can be used to calculate the abnormality misdetection probability. Let's first define the probability density function of vital signs heart rate, y_1, respiration rate, y_2 and oxygen saturation y_3. We assume

that the combined features $y = \gamma_1 y_1 + \gamma_2 y_2 + \gamma_3 y_3$ follow a Gaussian distribution with mean $\mu_n = \sum_{i=1}^{3} \mu_{n,i}\gamma_i$ and variance $\sigma_n^2 = \sum_{i=1}^{3} \sigma_{n,i}^2 \gamma_{n,i}^2$ for normal vital signs. Abnormal vital signs follow a Gaussian distribution with mean $\mu_a = \sum_{i=1}^{3} \mu_{a,i}\gamma_i$ and variance $\sigma_a^2 = \sum_{i=1}^{3} \sigma_{a,i}^2 \gamma_{a,i}^2$.

B. Accuracy Model

We set a detection threshold $\tau = \sum_{i=1}^{3} \tau_i \gamma_i$ over the thresholds $\{\tau_1, \tau_2, \tau_3\}$ for each feature dividing divides normal from abnormal vital signs. We, then, define $\mathcal{P}_{\text{DE}}$ as the misdetection probability of normal vs abnormal vital signs. In fact, the probability density functions of abnormal vital signs (e.g. $f_a(y|U, X)$) and error (e.g. $\rho(e|U, X)$ in Section III-B) follow independent Gaussian distributions.

Let $\mathcal{P}_{\text{DE}} = \mathcal{P}(\alpha, \beta, \eta)$ be the abnormality misdetection probability with the following events:

- sensor's error tolerance $\alpha = \{e(U, X) < \text{T}\}$,
- region of abnormal vital signs $\beta = \{y > \tau\}$, and
- activity and current level $\eta = \{X = x, U = u\}$.

The joint misdetection probability can be written as,

$$\mathcal{P}_{\text{DE}} = \mathcal{P}(\alpha \mid \beta, \eta)\mathcal{P}(\beta \mid \eta)\mathcal{P}(\eta). \tag{3}$$

Consider the upper bound for the $\mathcal{P}(\eta)$, with no prior knowledge about U and X,

$$\mathcal{P}_{\text{DE}} \leq \mathcal{P}(\alpha \mid \beta, \eta)\mathcal{P}(\beta|\eta). \tag{4}$$

Note that abnormal vital signs are functions of the activity but independent of sensor's current level,

$$\mathcal{P}_{\text{DE}} \leq \mathcal{P}(\alpha \mid \eta)\mathcal{P}(\beta \mid X = x) = \mathcal{P}_{\text{UB}}. \tag{5}$$

Assuming $\mathcal{P}(\alpha \mid \eta(U, X)) \sim \mathcal{N}(0, \sigma)$ and $\mathcal{P}(\beta \mid X = x) \sim \mathcal{N}(\mu_a, \sigma_a)$ we obtain

$$\mathcal{P}_{\text{UB}} = \int_{-\infty}^{T} \rho_E(\alpha \mid \eta) de \int_{\tau}^{\infty} f_a(\beta \mid X = x) dy. \tag{6}$$

By substituting error probability in the sensor from Eq. 2, we finally obtain

$$\mathcal{P}_{\text{UB}} = \mathcal{P}_{\text{error}}(T) \int_{\tau}^{\infty} f_a(\beta \mid X = x) dy. \tag{7}$$

We can now formulate the optimization problem as the trade off between sensing power consumption C_{TX} and the probability $\mathcal{P}_{\text{UB}}$ as follows

$$\begin{aligned} \underset{U}{\text{minimize}} \quad & C_{\text{TX}}(U) \\ \text{subject to} \quad & \mathcal{P}_{\text{UB}} \leq \theta \\ & \text{or, equivalently,} \\ & \mathcal{P}(\alpha \mid \eta) \leq \frac{\theta}{\mathcal{P}(\beta \mid X = x)} = \zeta. \end{aligned} \tag{8}$$

We define the Lagrangian multiplier λ to solve the equivalent optimization problem,

$$\mathcal{L}(U, \lambda) = C_{\text{TX}}(U) + \lambda(\mathcal{P}(\alpha \mid \eta) - \zeta). \tag{9}$$

Taking the derivative w.r.t. the sensor's current level,

$$\frac{\partial C_{\text{TX}}(U)}{\partial U} + \lambda \frac{\partial \mathcal{P}(\alpha \mid \eta)}{\partial U} = 0 \tag{10}$$

we obtain a linear relation between power consumption and current level:

$$a_U + \lambda \frac{\partial \mathcal{P}(\alpha \mid \eta)}{\partial \alpha} \frac{\partial \alpha}{\partial U} = 0. \tag{11}$$

Given the Gaussian PDF of α and linearity between α and U, we have

$$a_U + \lambda b_U \sum_{i=1}^{N} \mathbb{1}[U = U_i] \frac{\partial \Phi_i(\alpha)}{\partial \alpha} = 0 \tag{12}$$

The optimal (U^*, λ^*) can be then calculated as

$$\sum_{i=1}^{N} \mathbb{1}[U = U^*] \frac{\partial \Phi_i(\alpha)}{\partial \alpha} = -\frac{a_U}{\lambda^* b_U} \tag{13}$$

The edge processor periodically determines in real-time the lowest sensor's current setting such that the maximum error probability is below the desired threshold. Assuming N possible current levels, the complexity this search is $O(N)$. The algorithm is summarized in 1).

Algorithm 1 Sensor current control loop

```
procedure SOLUTION(τ, T)  ▷ τ and T are thresholds at a given time t
    Extract Activity level X
    for U ∈ {U_1, ..., U_5} do
        Calculate the variance of the error e(U, X).
        Calculate tail Gaussian P(e | U = u, X = x)
        Estimate P_DE using P_UB.
        if P_UB < τ then return u
        else
            continue
    until the system is terminated
```

IV. Numerical Results

We now illustrate the characteristics of the vital sign signals and the performance of the proposed system. We use the total variance of $RMSE$ to determine the parameters of the Gaussian distribution modeling misdetection. As shown in Figure 5 (a), as expected the variance decreases when the current level is increased. This is more apparent in vigorous activities, such as "Jogging" or "Running".

Figure 6 shows the PDF of two activities with the calculated error variance. Higher values of variance in lower current levels lead to higher values of the error probability P_{error}. The shaded regions in Figures 6 (a) and 6 (b) correspond to P_{error} with a threshold of $RMSE$, $T = 2$ (see Section III-B). Note that the error probability in vigorous states decreases significantly with higher current levels. We observe that the error probability during "Running" or "Jogging" with the minimum current level of $0.8mA$ is one. In other words, none of the features, including heart rate, respiration rate or

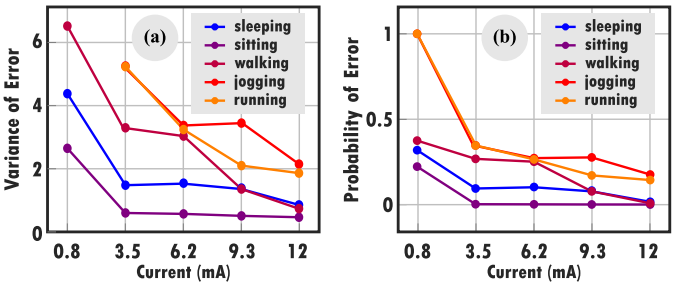

Fig. 5: (a) Total Error variance for different activity X and current level U. (b) Error probability for different activity X and current level U with maximum $RMSE = 2$

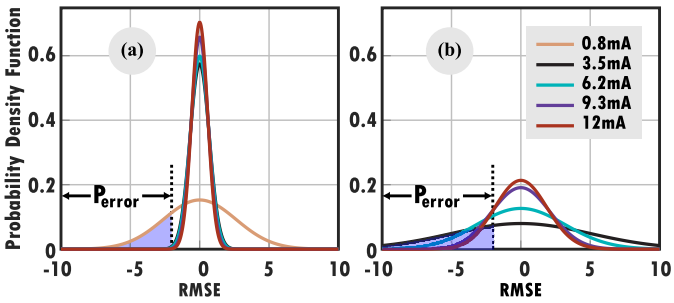

Fig. 6: Error probability when $RMSE = 2$ for different current levels during two states: (a) sitting, (b) running

SpO_2 can be extracted from the noisy signal. High noise levels often affect signal acquisition in wearable devices when users engage in vigorous physical activities. In our system, the consequence is that of $3.5mA$ is the lowest acceptable current level is such activities.

In order to evaluate our edge-assisted control platform, a healthy individual was monitored for 24-hour. The user's physical activity is estimated using the 3D acceleration signal. Placing the accelerometer sensor at the user's hand, we use hand movements to extract user's steps. The acceleration data is filtered, and steps are counted in each time interval. In addition, when no steps are detected, the orientation of the user is leveraged to differentiate between sitting and sleeping activities. Figure 7 (a) shows the activity level labeled "Sleeping", "Sitting", "Walking", "Jogging" and "Running" as $\{1, 2, 3, 4, 5\}$ respectively.

Considering $T = 2$ as the predefined threshold of $RMSE$, we calculated the error probability for each current level. At each given time, based on the activity level, we are able to choose the lowest current level that satisfies the misdetection probability $\mathcal{P}_{\text{UB}}$ shown in Equation 8. High activity levels necessitate accurate monitoring that require choosing high current levels.

In contrast, low activity levels, can fulfill the same threshold of probability of error with lower current levels. In the experiment shown in Figure 7 (a), we set the maximum probability of error to $\zeta = 0.17$ and set the weights as $\gamma_1 = 0.25, \gamma_2 = 0.35, \gamma_3 = 0.4$. In the results, we define the mean and variance of abnormal vital signs for each activity. In particular, the aggregate of normal vital signs y follows the distribution $\mathcal{N}(\mu_n, \sigma_n)$ with $\mu_n = \{57.72, 60.43, 74.29, 83.97, 91.53\}$ and $\sigma_n = \{0.25, 0.73, 1.17, 1.45, 0.62\}$ in the order of "Sleeping", "Sitting", "Walking", "Jogging" and "Running", respectively.

In case of abnormal vital signs, y follows $\mathcal{N}(\mu_a, \sigma_a)$ with $\mu_a = \{56.83, 61.07, 74.15, 81.50, 97.00\}$ and $\sigma_a = \{2.02, 0.71, 2.29, 1.67, 2.88\}$, respectively. The threshold τ in Equation 6 is the intersection of two Gaussian distributions for each activity. The probability of abnormal vital signs is calculated using the Cumulative Distribution Function (CDF) with $\tau = \{57.20, 60.73, 72.76, 82.68, 89.58\}$. Based on this parameters, the probability $\mathcal{P}(\beta \mid X = x) = \{0.57, 0.68, 0.72, 0.76, 0.99\}$ is then calculated according to Equation 6. Based the predefined threshold $\zeta = 0.17$ in error probability of sensor and $\mathcal{P}(\beta \mid X = x)$, we calculate the new

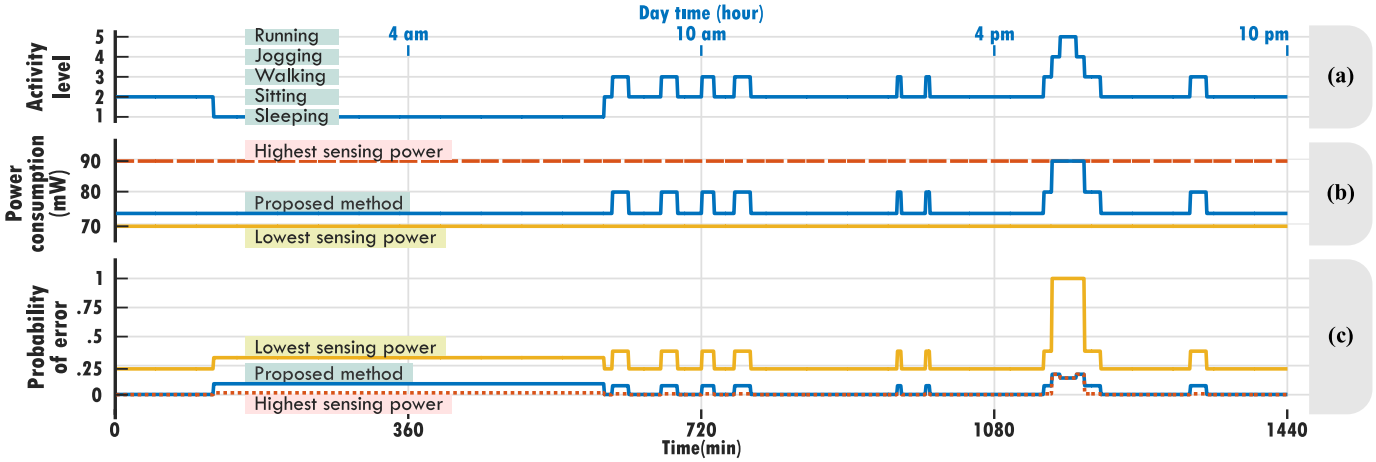

Fig. 7: 24-hour health monitoring of a healthy person. (a) user's activity level. (b) sensor's sensing power consumption. (c) Error probability in abnormality detection expected regarding the user's activity. The red line, yellow line and blue line indicate the baseline of highest, lowest and our proposed platform sensing power consumption, respectively.

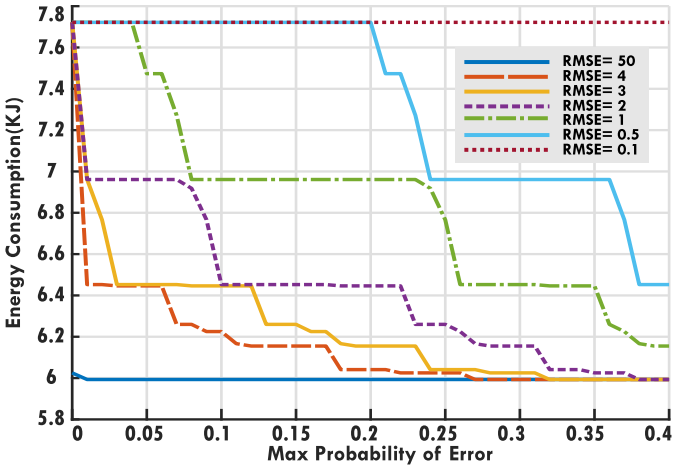

Fig. 8: Sensing energy consumption as a function of maximum probability of error with different RMSE levels.

threshold for the probability of misdetection to fulfill the upper bound $\theta = \zeta \times \mathcal{P}(\beta \mid X = x)$ (see Equation 8). The threshold $\theta = \{0.09, 0.11, 0.12, 0.13, 0.17\}$ corresponds to the desired upper bound of misdetection probability $\mathcal{P}_{\text{UB}}$ for each activity.

Figure 7 (b) illustrates the comparison between our proposed methodology, and static current levels corresponding to the lowest and the highest sensing power. The lowest sensing power consumption in the sensor leads to unacceptably high error probability, while the highest current level leads to an excessively high energy consumption. During the 24-hour experiment, we measured 5983.4J and 7721.4J consumed by the lowest and highest sensing power, respectively. Our energy efficient algorithm reduced the energy consumption to 6417.5J. Average sensing power consumption of 74.32mW was observed which amounts to a 16.9% reduction compared to 89.43mW of the highest sensing power level. Figure 7 (c) shows the error probability associated with each current level. Note that using the lowest current level leads to an unacceptable $P_{error} = 1$ during "Jogging" and "Running".

Using the same scenario of 24-hour activity, we measured the tradeoff between the maximum error probability and energy consumption, which is illustrated in Figure 8. Our system can detect abnormalities with tolerance of $RMSE = 50$ by choosing the lowest current level, leading to an energy expense equal to 5983.4J. If we set the maximum error tolerance to $RMSE = 0.1$ or less, we have a large probability of error for all current levels during any activity. Therefore, no matter what we determine as the maximum error probability threshold, the system will choose the highest current level and the total sensing energy consumption during a 24- hour activity monitoring is 7721.4J. Settings between these two extreme cases determine the maximum probability of error and the necessary energy consumption. The energy expense over the 24h period decreases as the maximum tolerable probability increases. Similarly, reducing the tolerable $RMSE$ variance decreases energy expense.

V. Conclusions

This paper proposes a context-aware control system for healthcare applications. The IoT infrastructure, and in particular edge and cloud servers, assist local sensors to dynamically adapt sensing parameters. The use-case we considered focuses on abnormality detection using PPG signals. We demonstrated that by adapting sensing accuracy, and thus energy consumption, to the user's activity, the lifetime of the sensor can be considerably extended. We leave to future work the development of predictive control strategies evaluating the long-term trajectory of users' daily activities.

Acknowledgements

This work was partially supported by the US National Science Foundation (NSF) WiFiUS grant CNS-1702950 and Academy of Finland grants 311764 and 311765.

References

[1] S. R. Islam, D. Kwak, M. H. Kabir, M. Hossain, and K.-S. Kwak, "The internet of things for health care: a comprehensive survey," *IEEE Access*, vol. 3, pp. 678–708, 2015.

[2] F. Bonomi *et al.*, "Fog computing and its role in the internet of things," in *Proceedings of the first edition of the MCC workshop on Mobile cloud computing*, 2012.

[3] A. M. Rahmani *et al.*, *Fog Computing in the Internet of Things - Intelligence at the Edge*. Springer, 2017.

[4] Y. Chen *et al.*, "Transmission scheduling for optimizing sensor network lifetime: A stochastic shortest path approach," *IEEE Transactions on Signal Processing*, vol. 55, no. 5, 2007.

[5] J. L. Williams *et al.*, "Approximate dynamic programming for communication-constrained sensor network management," *IEEE Transactions on signal Processing*, 2007.

[6] L. Wang and Y. Xiao, "A survey of energy-efficient scheduling mechanisms in sensor networks," *Mobile Networks and Applications*, 2006.

[7] A. Aijaz and A. H. Aghvami, "Cognitive machine-to-machine communications for internet-of-things: A protocol stack perspective," *IEEE Internet of Things Journal*, vol. 2, no. 2, pp. 103–112, 2015.

[8] G. Fang and E. Dutkiewicz, "Bodymac: Energy efficient tdma-based mac protocol for wireless body area networks," in *ISCIT 2009. 9th International Symposium on*. IEEE, 2009.

[9] S. A. Gopalan and J.-T. Park, "Energy-efficient mac protocols for wireless body area networks: survey," in *ICUMT*. IEEE, 2010.

[10] D. Zois *et al.*, "A pomdp framework for heterogeneous sensor selection in wireless body area networks," in *INFOCOM*, 2012, pp. 2611–2615.

[11] D. Zois *et al.*, "Active classification for pomdps: A kalman-like state estimator," *IEEE Transactions on Signal Processing*, 2014.

[12] D. Zois *et al.*, "Energy-efficient, heterogeneous sensor selection for physical activity detection in wireless body area networks," *IEEE Transactions on signal processing*, 2013.

[13] A. M. Rahmani *et al.*, "Exploiting smart e-health gateways at the edge of healthcare internet-of-things: a fog computing approach," *Future Generation Computer Systems*, vol. 78, no. 2, pp. 641–58, 2018.

[14] A. Hertzman, "The blood supply of various skin areas as estimated by the photoelectric plethysmograph," *American Journal of Physiology*, 1938.

[15] P. Charlton *et al.*, "An assessment of algorithms to estimate respiratory rate from the electrocardiogram and photoplethysmogram," *Physiol Meas.*, 2016.

[16] W. Karlen *et al.*, "Multiparameter respiratory rate estimation from the photoplethysmogram," *IEEE Transactions on Biomedical Engineering*, 2013.

[17] A. Garde *et al.*, "Estimating respiratory and heart rates from the correntropy spectral density of the photoplethysmogram," *PLoS One*, 2014.

[18] L. Lindberg *et al.*, "Monitoring of respiratory and heart rates using a fibre-optic sensor," *Med. Biol. Eng. Comput.*, vol. 30, pp. 533–7, 1992.

[19] Maxim Integrated, , (accessed 2018-08-01), https://www.maximintegrated.com/en/products/sensors/MAX30102.html.